

## EARTHQUAKE PERFORMANCE OF STEEL FRAMES WITH NITINOL BRACES

FERDINANDO AURICCHIO<sup>†,‡,¶</sup>, DAVIDE FUGAZZA<sup>†,¶,\*</sup> and REGINALD DESROCHES<sup>§</sup>

<sup>†</sup>*Dipartimento di Meccanica Strutturale  
Università degli Studi di Pavia  
Via Ferrata 1, 27100 Pavia, Italy*

<sup>‡</sup>*Istituto di Matematica Applicata e Tecnologie Informatiche  
Università degli Studi di Pavia  
Via Ferrata 1, 27100 Pavia, Italy*

<sup>¶</sup>*European School for Advanced Studies in Reduction of Seismic Risk  
(ROSE School) Via Ferrata 1, 27100 Pavia, Italy*

<sup>§</sup>*School of Civil and Environmental Engineering  
Georgia Institute of Technology  
790 Atlantic Drive, Atlanta, GA 30332-0355, USA*

In this paper, the seismic performance of a three- and a six-storey steel frame equipped with different bracing configurations is assessed. The bracing systems consist of traditional buckling-restrained steel braces and superelastic Nitinol shape-memory alloy (SMA) braces. Background on the behaviour of SMAs is provided and a state-of-the-art review of the applications of such new materials in earthquake engineering is presented. A uniaxial constitutive model for superelastic SMAs is then implemented into the finite element platform OpenSees and nonlinear dynamic analyses are performed. Finally, the seismic performance of the structures under investigation is judged through the evaluation of several response quantities, to determine the efficacy of the new bracing system in reducing earthquake-induced vibrations.

*Keywords:* Shape-memory alloys; steel frames; bracing systems; dynamic analyses; seismic applications.

### 1. Introduction

Shape-memory alloys (SMAs) are a class of alloy with characteristics not present in materials traditionally used in civil engineering. At the macroscopic level, SMAs feature two unique properties: *superelasticity* and *shape-memory effect*. The former is related to the ability of recovering large deformations after removal of the external load and the latter is the capacity to regain the original shape by means of thermal cycles [Duerig *et al.*, 1990].

Due to their unique behaviour, SMAs have attracted significant attention in recent years from the scientific community. SMAs have been widely used in many different fields, including aerospace, automotive and biomedical applications. Also,

\*Currently at SAMTECH Italia s.r.l., Via Giovanni Rasori 13, 20145 Milano, Italy

recent numerical and experimental investigations have highlighted the possibility of utilising such materials as innovative seismic devices for the protection of buildings and bridges [DesRoches and Smith, 2004; Wilson and Wesolowsky, 2005].

Although the existing literature provides a number of analytical studies regarding the use of SMA-based devices, little research has been carried out in terms of structural applications of large cross-section SMA elements in earthquake engineering. In this respect, this paper focuses on the use of large diameter superelastic SMA bars in innovative bracing systems for steel buildings. In particular, computer simulations are conducted to compare the seismic response of a three- and a six-storey steel frame building equipped with two different bracing configurations: traditional buckling-restrained steel braces and superelastic SMA braces.

## 2. Innovative Structural Materials: Shape-Memory Alloys

The unique properties of SMAs are related to reversible martensitic phase transformations, that is, solid-to-solid diffusionless processes between a crystallographically more-ordered phase, *austenite*, and a crystallographically less-ordered phase, *martensite*. The latter may be present in single or multiple *variants*.<sup>a</sup> Typically, the austenite is stable at low stresses and high temperatures, while the martensite is stable at high stresses and at low temperatures. These transformations can be either thermal-induced or stress-induced [Duerig *et al.*, 1990].

### 2.1. Phase transformations

In the stress-free state, an SMA is characterised by four transformation temperatures:  $M_s$  and  $M_f$  during cooling and  $A_s$  and  $A_f$  during heating. The former two (with  $M_s > M_f$ ) indicate the temperatures at which the transformation from the austenite into martensite, also named as *parent phase*, respectively starts and finishes, while the latter two (with  $A_s < A_f$ ) are the temperatures at which the inverse transformation, also named as *reverse phase*, respectively starts and finishes.

### 2.2. Superelasticity and shape-memory effect

The phase transformations between austenite and martensite are the keys to explain the superelasticity and the shape-memory effect. For the simple case of uniaxial tensile stress, a brief explanation follows.

<sup>a</sup>The martensite can be present in different but crystallographically equivalent forms (variants). If there is no preferred direction along which the martensite variants tend to align, then multiple variants are formed. If, instead, there is a preferred direction for the formation of martensite, just one (single) variant is formed.

- **Superelasticity** (Fig. 1). Consider a specimen in the austenitic state and at a temperature greater than  $A_f$ ; accordingly, at zero stress only the austenite is stable. If the specimen is loaded, while keeping the temperature constant, the material presents a nonlinear behaviour ( $ABC$ ) due to a stress-induced conversion of austenite into single-variant martensite. Upon unloading, while again keeping the temperature constant, a reverse transformation from single-variant martensite to austenite occurs ( $CDA$ ) as a result of the instability of the martensite at zero stress. At the end of the loading-unloading process no permanent strains are present and the stress-strain path is a closed hysteresis loop.
- **Shape-memory effect** (Fig. 2). Consider a specimen in the multiple-variant martensitic state and at temperature lower than  $M_s$ ; accordingly, at zero stress

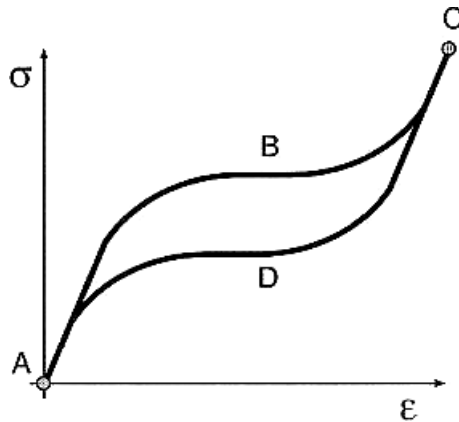


Fig. 1. Superelasticity. At a constant high temperature the material is able to undergo large deformations with zero final permanent strain. Note the closed hysteresis loop.

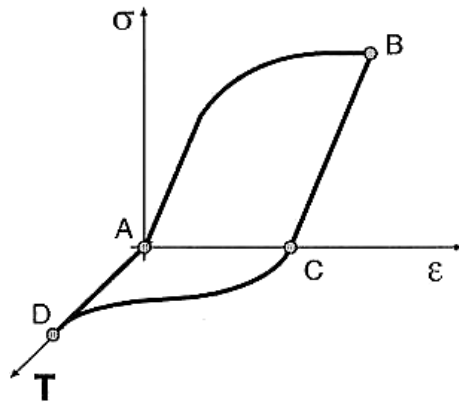


Fig. 2. Shape-memory effect. At the end of a loading-unloading path ( $ABC$ ) performed at a constant low temperature, the material presents residual deformations ( $AC$ ) which can be recovered through a thermal cycle ( $CDA$ ).

only the martensite is stable, either in a single-variant or in a multiple-variant composition. During loading, the material has a nonlinear response ( $AB$ ) due to a stress-induced conversion of the multiple-variant martensite into a single-variant martensite. During unloading ( $BC$ ) residual deformations appear ( $AC$ ). However, the residual strain may be recovered by heating the material to a temperature above  $A_f$ , thus inducing a temperature-driven conversion of martensite into austenite. Finally, upon cooling, the austenite is converted back into multiple-variant martensite.

### 2.3. An example of shape-memory alloy material: Nitinol

The *nickel-titanium*<sup>b</sup> (NiTi) system is based on the equiatomic compound of nickel and titanium. Nitinol SMAs have the ability to undergo large recoverable strains, typically on the order of 3 to 6%, possess high stability in cyclic applications and are highly corrosion resistant (Table 1).

For commercial exploitation, and in order to improve its properties, a third metal is usually added to the binary system. In some cases, a nickel quantity up to an extra 1% is added. This increases the yield strength of the austenitic phase while simultaneously suppressing the transformation temperatures.

The manufacturing process of NiTi alloys is difficult due to the hardness of the material, then resulting in an increased cost of its use. Anyway, despite this disadvantage, the excellent mechanical properties of NiTi alloys (Table 2) have made them the most frequently used SMA material in commercial applications.

Table 1. Properties of binary Nitinol SMAs.

|                                    |                           |
|------------------------------------|---------------------------|
| Melting temperature                | 1300 [°C]                 |
| Density                            | 6.45 [g/cm <sup>3</sup> ] |
| Resistivity of austenite           | ≈ 100 [μΩ · cm]           |
| Resistivity of martensite          | ≈ 70 [μΩ · cm]            |
| Thermal conductivity of austenite  | 18 [W/(cm · °C)]          |
| Thermal conductivity of martensite | 8.5 [W/(cm · °C)]         |
| Corrosion resistance               | similar to Ti alloys      |
| Young's modulus of austenite       | 25 000–70 000 [MPa]       |
| Young's modulus of martensite      | 20 000–50 000 [MPa]       |
| Yield strength of austenite        | 200–700 [MPa]             |
| Yield strength of martensite       | 70–140 [MPa]              |
| Ultimate tensile strength          | ≈ 900 [MPa]               |
| Transformation temperature         | –200–110 [°C]             |
| Shape-memory strain                | 8.5 [%]                   |

<sup>b</sup>Sometimes the nickel-titanium alloy is called Nitinol (pronounced night-in-all). The name represents its elemental components and place of origin. The “Ni” and “Ti” are the atomic symbols for nickel and titanium. The “NOL” stands for the Naval Ordnance Laboratory where it was discovered.

Table 2. Nitinol SMAs versus typical structural steel: comparison of the mechanical properties. Letters A and S stand for, respectively, austenite and martensite while abbreviations f.a. and w.h. respectively refer to the names “fully annealed” and “work hardened” which are two types of treatment.

| Property                  |       | Nitinol SMAs              | Steel   |
|---------------------------|-------|---------------------------|---------|
| Recoverable elongation    | [%]   | 5–8                       | 2       |
| Modulus of elasticity     | [MPa] | see Table 1               | 200 000 |
| Yield strength            | [MPa] | see Table 1               | 248–517 |
| Ultimate tensile strength | [MPa] | 900 (f.a.), 2000 (w.h.)   | 448–827 |
| Elongation at failure     | [%]   | 25–50 (f.a.), 5–10 (w.h.) | 20      |
| Corrosion performance     | [–]   | Excellent                 | Fair    |

### 3. Use of Shape-Memory Alloys in Earthquake Engineering: A State-of-the-Art Review

This section presents an updated state-of-the-art review of the applications of the SMA technology in earthquake engineering, where such innovative materials are being considered as both vibration control devices and isolation systems for the seismic protection of buildings and bridges.

#### 3.1. Numerical applications

Wilde *et al.* [2000] proposed a smart isolation system for bridge structures which combined a laminated rubber bearing with a device made of SMA bars attached to the pier and the superstructure. The new device was mathematically modelled and analytically studied for earthquakes with different accelerations. For the smallest earthquake, the system provided a stiff connection between the pier and the deck. For the medium earthquake, the SMA bars provided increased damping capabilities to the system due to the stress-induced martensite transformation of the alloy. Finally, for the largest seismic event, the SMA bars provided hysteretic damping and acted as a displacement control device due to the hardening of the alloy after the phase transformation was completed.

Bruno and Valente [2002] presented a comparative analysis of different passive seismic protection strategies, aimed at quantifying the improvement achievable with the use of innovative devices based on SMAs in place of traditional steel or rubber devices (i.e. bracing and base isolation systems). The researchers found that SMA-based devices were more effective than rubber isolators in reducing seismic vibrations. On the other hand, the same conclusions could not be drawn for SMA braces if compared to steel braces because of the similar structural performance. However, SMA braces proved preferable considering the recentring capabilities not possessed by steel braces as well as the reduced functional and maintenance requirements.

Baratta and Corbi [2002] and Corbi [2003] investigated the influence of SMA tendon elements used to improve the overall strength of a simple portal frame model undergoing horizontal shaking. Numerical results showed that the structure

endowed with superelastic tendons considerably improved the dynamic response with respect to the case in which the tendons were made of elastic-plastic wires. SMA tendons produced smaller response amplitude, much smaller residual drift and excellent performance in attenuating P- $\Delta$  effects.

DesRoches and Delemont [2002] considered the application of superelastic SMA restrainers to a multi-span bridge. The SMA restrainers were connected from the pier cap to the bottom flange of the beam in a manner similar to typical cable restrainers. The results showed that the proposed system reduced relative hinge displacements at the abutment much more effectively than conventional steel cable restrainers. The large elastic strain range of the SMA device allowed it to undergo large deformations while remaining elastic. In addition, the superelastic properties of the SMA restrainers resulted in energy dissipation at the hinges. Also, for unexpected strong earthquakes, the increased stiffness that SMAs exhibit at large strains provided additional restraint to limit the relative openings in the bridge.

### **3.2. *Experimental applications***

Clark *et al.* [1995] performed an extensive testing program on a wire-based SMA devices to evaluate the effects of temperature and loading frequency on their cyclic behaviour. The devices used a basic configuration of multiple loops of superelastic wires wrapped around cylindrical supports. Two pairs of devices were tested and each of the four devices had identical hardware but different wire configuration. The proposed dampers exhibited stable hysteresis with minor variations due to frequency of loading and device configuration (single layer versus multiple layers of wires). Moreover, the research highlighted that the temperature effects were substantial in the single-sided device.

Krumme *et al.* [1995] examined the performance of a sliding SMA device in which resistance to sliding was achieved by opposite pairs of SMA tension elements. Experimental results reported temperature insensitivity, frequency independence and excellent cyclic behaviour.

Adachi and Unjoh [1999] developed an energy dissipation device for bridges using SMA plates. The device was designed to take the load only in bending and its damping characteristics were determined through both cycling loadings and shake table tests. Experiments successfully showed that the SMA damper, which worked as a cantilever beam, could reduce the seismic response of the bridge and that its performance was more effective and efficient if the utilised SMA material displayed the shape-memory effect.

Castellano [2000] and Indirli *et al.* [2000] realised different brick masonry wall mock-ups, simulating a portion of a cultural heritage structure, to be tested on the shake table. The aim of the experimental investigation was to evaluate the effectiveness of innovative techniques based on the use of SMAs as ties for the prevention of the out-of-plane collapse of such walls. Results from the tests showed that the

new tying system could be highly effective to prevent the out-of-plane collapse of peripheral walls, such as church façades, poorly connected at the floor level.

Dolce *et al.* [2000] studied in great detail the possibility of using special braces for framed structures utilising SMAs. Due to the extreme versatility of such materials, they could obtain a wide range of cyclic behaviour (from supplemental and fully recentring to highly dissipating) by simply varying the number and/or the characteristics of the SMA components. In particular, they proposed three categories of devices: supplemental re-centring devices, not re-centring devices and re-centring devices.

The idea of using a SMA-based bracing system as a damper device for the structural vibration control of a frame was also considered by Han *et al.* [2003]. They carried out an experimental test on a two-storey steel frame endowed with eight SMA dampers. The researchers focused on free-vibrations, concentrating on the decay history shown by the frame with and without the SMA dampers. Results highlighted that the frame equipped with the innovative bracing system took much shorter time to reduce its initial displacement than the uncontrolled frame (i.e. frame without the dampers).

Ocel *et al.* [2004] evaluated the feasibility of a new class of partially restrained connections by using SMAs in their martensitic form. The proposed connection consisted of four large diameter SMA bars connecting the beam flange to the column flange and served as the primary moment transfer mechanism. Under cyclic loadings, the connection exhibited a high level of energy dissipation, large ductility capacity and no strength degradation. Following the initial testing series, the tendons were then heated above the transformation temperature to evaluate the potential for recovering the residual deformation. The connection was then retested and exhibited nearly identical behaviour to the original one with repeatable and stable hysteretic behaviour.

Dolce *et al.* [2005] performed shake table tests on reduced-scale RC frames endowed with either steel or SMA braces. The experimental outcomes showed that the new bracing system based on SMAs may provide performances at least comparable to those provided by currently used devices, also in the absence of design criteria and methods specifically addressed to the new technology. With respect to steel braces, the innovative bracing configuration presented excellent fatigue resistance and recentring ability.

### 3.3. Existing applications

The Basilica of St. Francis in Assisi was severely damaged during the 1999 earthquake occurred in central Italy [Crocì *et al.*, 2000; Mazzolani and Mandara, 2002]. The main challenge of the restoration was to obtain an adequate safety level while maintaining the original concept of the structure. In order to reduce the seismic forces transferred to the tympanum, a connection between it and the roof was created using superelastic SMA wires.

The rehabilitation of the bell tower of the church of San Giorgio in Trignano, Italy, is another important example of seismic retrofit utilising SMAs [Indirli, 2000; Mazzolani and Mandara, 2002]. The structure is very old (XIV century), is made of masonry and it was seriously damaged during the 1996 earthquake. The innovative intervention consisted in the insertion of four vertical prestressing steel tie bars placed in series with four SMA devices made of superelastic wires.

#### 4. A Uniaxial Constitutive Model for Superelastic Shape-Memory Alloy Braces

For representing the superelastic behaviour of SMA braces, we choose the constitutive model described in the work by Fugazza [2003]. Such a model, which is a modification of the one proposed by Auricchio and Sacco [1997], is capable of describing the material behaviour under arbitrary loadings, such as those involved in seismic excitations, where the response is mainly composed by sub-hysteresis loops internal to the main one associated with complete phase transformations. The model formulation, developed in the small deformation regime, relies on the assumption that the relationship between stresses and strains is represented by a series of straight lines whose form is determined by the extent of the transformation experienced. Further assumptions made, in agreement with previous studies, are that no strength degradation occurs during cycling [Bernardini and Brancaleoni, 1999] and that austenite and martensite branches have the same modulus of elasticity [Andrawes *et al.*, 2004].

##### 4.1. *Time-continuous model*

We propose to work with one scalar internal variable,  $\xi_S$ , representing the *martensite fraction*, and with two processes which may produce its variation:

- the conversion of austenite into martensite ( $A \rightarrow S$ ),
- the conversion of martensite into austenite ( $S \rightarrow A$ ).

For both processes, we choose linear *kinetic rules* to describe the evolution in time of the martensite fraction. In particular, the activation conditions for the conversion of austenite into martensite are:

$$\sigma_s^{AS} < |\sigma| < \sigma_f^{AS} \quad \text{and} \quad \overline{|\dot{\sigma}|} > 0, \quad (1)$$

where  $\sigma_s^{AS}$  and  $\sigma_f^{AS}$  are material parameters representing the stress levels at which the  $A \rightarrow S$  transformation starts and finishes respectively,  $|\cdot|$  is the absolute value and a superpose dot indicates a time derivative.<sup>c</sup> The corresponding evolutionary equation is set equal to:

$$\dot{\xi}_S = -(1 - \xi_S) \frac{\overline{|\dot{\sigma}|}}{|\sigma| - \sigma_f^{AS}}. \quad (2)$$

<sup>c</sup>A superposed dot over a bar indicates that the whole quantity under the bar is derived.

On the other hand, the activation conditions for the conversion of martensite into austenite are:

$$\sigma_f^{SA} < |\sigma| < \sigma_s^{SA} \quad \text{and} \quad \dot{|\sigma|} < 0, \quad (3)$$

where  $\sigma_f^{SA}$  and  $\sigma_s^{SA}$  are material parameters representing the stress levels at which the S  $\rightarrow$  A transformation starts and finishes respectively. The corresponding evolutionary equation is set equal to:

$$\dot{\xi}_S = \xi_S \frac{\dot{|\sigma|}}{|\sigma| - \sigma_f^{SA}}. \quad (4)$$

Limiting the discussion to a small deformation regime, we assume the following additive decomposition of the total strain  $\epsilon$ :

$$\epsilon = \epsilon^e + \epsilon_L \xi_S \text{sgn}(\sigma), \quad (5)$$

where  $\epsilon^e$  is the elastic strain,  $\epsilon_L$  is the maximum residual strain and  $\text{sgn}(\cdot)$  is the sign function.

Finally, the elastic strain is assumed to be linearly related to the stress:

$$\sigma = E \epsilon^e, \quad (6)$$

with  $E$  the elastic modulus of both the austenitic and martensitic branch.

#### 4.2. Time-discrete model

During the development of the time-continuous model we assumed the stress as control variable. However, in the development of the time-discrete model we assume the strain as control variable. The choice is consistent with the fact that, from the point of view of the integration scheme, the time-discrete problem is considered as strain-driven.

Accordingly, we consider two time values,  $t_n$  and  $t_{n+1} > t_n$ , such that  $t_{n+1}$  is the first time value of interest after  $t_n$ . Then, knowing the strain at time  $t_{n+1}$  and the solution at time  $t_n$ , we should compute the new solution at time  $t_{n+1}$ . With the aim of minimising the appearance of subscripts, we introduce the convention:

$$\alpha_n = \alpha(t_n), \quad \alpha = \alpha(t_{n+1}),$$

where  $\alpha$  is a generic quantity. As a consequence, the subscript  $n$  indicates a quantity evaluated at time  $t_n$ , while no subscript indicates a quantity evaluated at time  $t_{n+1}$ .

We then use a backward-Euler scheme for the integration of the time-continuous evolutionary Eqs. (2) and (4). Written in residual form and after clearing the fractions, the time-discrete evolutionary equations specialise to:

$$\mathcal{R}^{AS} = \lambda_S (|\sigma| - \sigma_f^{AS}) + (1 - \xi_S) (|\sigma| - |\sigma_n|) = 0, \quad (7)$$

$$\mathcal{R}^{SA} = \lambda_S (|\sigma| - \sigma_f^{SA}) - \xi_S (|\sigma| - |\sigma_n|) = 0, \quad (8)$$

where the martensite fraction increment,  $\lambda_S$ , is defined as:

$$\xi_S = \xi_{S,n} + \lambda_S \quad \text{or} \quad \lambda_S = \int_{t_n}^{t_{n+1}} \dot{\xi}_S dt. \quad (9)$$

Making use of Eq. (5), substitution of Eq. (6) into Eqs. (7) and (8) transforms the time-discrete evolutionary equations in two expressions which can be solved in terms of  $\lambda_S$ , which is the only unknown.

### 4.3. *Considerations on the adopted constitutive model*

We dedicate this section to the discussion of the adopted constitutive model. For brevity, we only indicate its advantages and disadvantages referring the reader to the work by Fugazza [2003] for the numerical assessment and for detailed information on the algorithmic solution. The main advantages of the adopted model are:

- robustness and simplicity of implementation,
- material parameters easy to obtain from typical uniaxial tests conducted on either wires or bars,
- ability to reproduce partial (i.e. sub-loops) and complete transformation patterns (i.e. from fully austenite to fully martensite) in both tension and compression.

However, the model has the following drawbacks:

- rate- and temperature-independence,
- inability to account for the different elastic properties between austenite and martensite.

## 5. Earthquake Records and Frame Characteristics

As far as the ground motions are concerned, a suite of 20 records developed for the SAC Steel Project [Sabelli, 2001], in particular for the Los Angeles area (California, USA), is used in this study. This consists of twenty seismic inputs with a 10% probability of exceedance in a 50-year period which were derived from historical recordings or from simulations of physical fault rupture processes. Later, for the numerical simulations, they will be scaled based on the average spectral acceleration of all twenty at the fundamental period of the frame under consideration.

Among the several steel buildings analysed by Sabelli [2001], two of them are considered. In particular, we concentrate on one three-storey frame and one six-storey frame, both designed to carry buckling-restrained steel braces oriented in a stacked chevron (inverted V) pattern. Geometric dimensions of the structures are given in Fig. 3, while member sizes are provided in Tables 3 and 4.

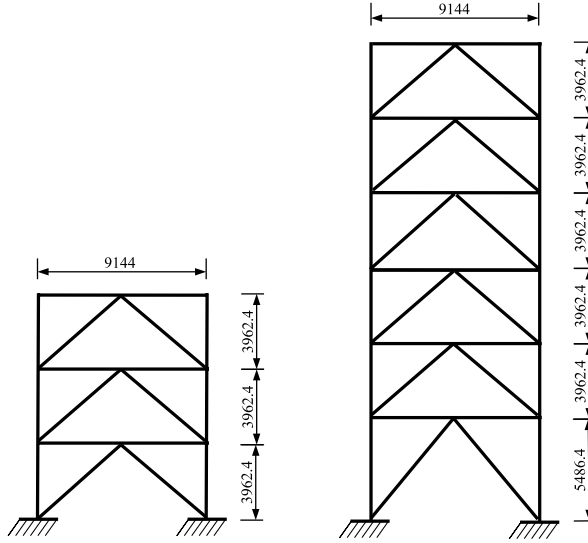


Fig. 3. Elevation view of the three- and six-storey frame. Dimensions are expressed in mm.

Table 3. Model information of the three-storey frame equipped with buckling-restrained steel braces (frame 3BR).

| Storey | Element size |           |                     |                      |
|--------|--------------|-----------|---------------------|----------------------|
|        | Column       | Beam      | Brace<br>$F_y$ [kN] | Brace<br>$K$ [kN/mm] |
| 1      | W 12 × 96    | W 14 × 48 | 1441                | 254                  |
| 2      | W 12 × 96    | W 14 × 48 | 1152                | 219                  |
| 3      | W 12 × 96    | W 14 × 48 | 698                 | 139                  |

Table 4. Model information of the six-storey frame equipped with buckling-restrained steel braces (frame 6BR).

| Storey | Element size |           |                     |                      |
|--------|--------------|-----------|---------------------|----------------------|
|        | Column       | Beam      | Brace<br>$F_y$ [kN] | Brace<br>$K$ [kN/mm] |
| 1      | W 14 × 211   | W 14 × 48 | 2273                | 334                  |
| 2      | W 14 × 211   | W 14 × 48 | 1730                | 330                  |
| 3      | W 14 × 211   | W 14 × 48 | 1552                | 299                  |
| 4      | W 14 × 132   | W 14 × 48 | 1410                | 274                  |
| 5      | W 14 × 132   | W 14 × 48 | 1281                | 251                  |
| 6      | W 14 × 132   | W 14 × 48 | 770                 | 156                  |

## 6. Finite Element Platform and Modelling Assumptions

Nonlinear dynamic analyses are performed by use of the Open System for Earthquake Engineering Simulation [Mazzoni *et al.*, 2003] framework. OpenSees is a PEER-sponsored project aimed at the development of a software platform able

to simulate the seismic response of structural and geotechnical systems. It is an open source code and, among its features, allows the users to implement their own material model.

Beams and columns are modelled using *nonlinearBeamColumn* elements with fibre sections and, apart from the roof level where there are hinges between the columns and the beams, fixed connections are assumed among elements. Braces are pinned at both ends so that they can ideally carry axial loads only. P- $\Delta$  effects are taken into consideration. Also, a 5% Rayleigh damping is specified, according to the typical values adopted for steel construction.

The uniaxial material model *steel01* is chosen for modelling beams, columns, and buckling-restrained steel braces. Mechanical properties of structural steel, such as elastic modulus,  $E^{steel}$ , and yielding stress,  $\sigma_y$ , are assumed to be the same as the ones considered by Sabelli [2001] and Sabelli *et al.* [2003], and are summarised in Table 5.

As previously mentioned, the adopted constitutive equation for superelastic SMAs is implemented into the OpenSees software to simulate the response of superelastic SMA braces. With respect to its original version, developed using the

Table 5. Material properties of structural steel and SMAs adopted for the numerical simulations.

| Parameter                  | Value   |
|----------------------------|---------|
| $E^{steel}$ [MPa]          | 200 000 |
| $E^{SMA}$ [MPa]            | 27 579  |
| $\sigma_y^{braces}$ [MPa]  | 250     |
| $\sigma_y^{beams}$ [MPa]   | 345     |
| $\sigma_y^{columns}$ [MPa] | 345     |
| $\sigma_s^{AS}$ [MPa]      | 414     |
| $\sigma_f^{AS}$ [MPa]      | 550     |
| $\sigma_s^{SA}$ [MPa]      | 390     |
| $\sigma_f^{SA}$ [MPa]      | 200     |
| $\epsilon_L$ [%]           | 3.50    |

Table 6. Geometry of the superelastic SMA braces for the three- and six-storey frame.

| Storey | SMA braces for frame 3BR |                         | SMA braces for frame 6BR |                         |
|--------|--------------------------|-------------------------|--------------------------|-------------------------|
|        | Length [mm]              | Area [mm <sup>2</sup> ] | Length [mm]              | Area [mm <sup>2</sup> ] |
| 1      | 378                      | 3481                    | 453                      | 5491                    |
| 2      | 351                      | 2783                    | 349                      | 4180                    |
| 3      | 336                      | 1687                    | 346                      | 3750                    |
| 4      | —                        | —                       | 343                      | 3406                    |
| 5      | —                        | —                       | 340                      | 3094                    |
| 6      | —                        | —                       | 330                      | 1859                    |

MATLAB environment, the model required additional programming work for its coding into the new finite element platform.

### 7. Design of Superelastic Shape-Memory Alloy Braces

For comparison purposes, superelastic SMA braces are designed to provide the same yielding strength,  $F_y$ , and the same axial stiffness,  $K$ , as steel braces (Fig. 4). In this way, the structure with the innovative bracing system will have the same natural period of the one with steel braces and both SMA and steel elements will yield at the same force level. In order to guarantee such properties, the following steps are performed:

- (i) Obtain yielding force,  $F_y$ , and axial stiffness,  $K$ , of the steel brace under consideration from the original structural design.

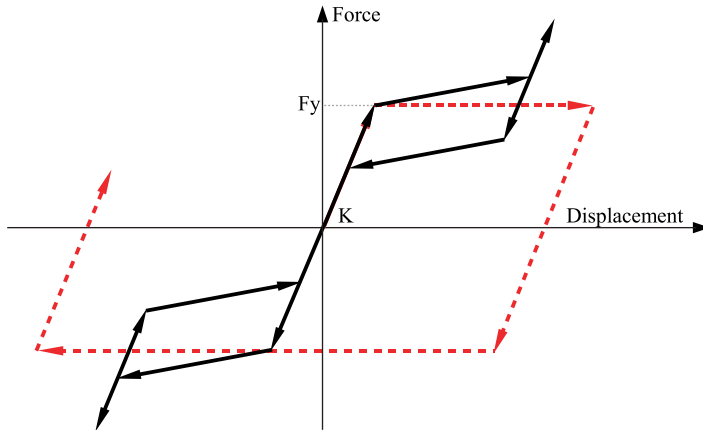


Fig. 4. Material models: buckling-restrained steel (dashed line) and superelastic SMAs (continuous line).

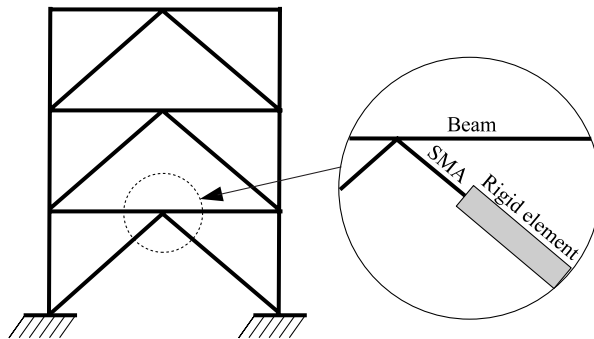


Fig. 5. Particular of the superelastic SMA brace installed in the three-storey frame.

- (ii) Obtain elastic modulus,  $E^{SMA}$ , of the considered SMA material and stress level,  $\sigma_s^{AS}$ , at which it enters the inelastic range (i.e. stress level to initiate the A  $\rightarrow$  S transformation).
- (iii) Compute area,  $A^{SMA}$ , of the corresponding SMA brace:

$$A^{SMA} = \frac{F_y}{\sigma_s^{AS}}. \quad (10)$$

- (iv) Compute length,  $L^{SMA}$ , of the corresponding SMA brace:

$$L^{SMA} = \frac{E^{SMA} A^{SMA}}{K}. \quad (11)$$

Table 6 shows the required geometric properties (i.e. element length and cross-sectional area) of the superelastic SMA braces. Since such members appear to be shorter than steel braces, in order to guarantee the actual brace length rigid elements are connected to each SMA member (Fig. 5). By doing so, we ensure all the deformation to occur in the SMA. Throughout this study, it is also assumed that the proposed smart braces are made of a number of large diameter superelastic Nitinol bars able to undergo compressive loads without buckling.

Their mechanical properties, provided in Table 5, are selected on the basis of the uniaxial tests carried out by DesRoches *et al.* [2004], who studied the cyclic behaviour of large diameter superelastic Nitinol bars for seismic applications. In particular, we choose those obtained from the dynamic tests, in order to correctly consider the reduced energy dissipation capability of such materials at high frequency loadings [Dolce and Cardone, 2001; DesRoches *et al.*, 2004; Fugazza, 2005].

## 8. Results and Discussion

In this section, the most important findings obtained from the nonlinear dynamic analyses of the structures under investigation are discussed.

First, we present and critically analyse selected results coming from a case study, then attention is paid to the computation of both the maximum interstorey drift and residual drift of the top floor, two quantities traditionally considered for the evaluation of the seismic performance of buildings undergoing earthquake motions.

Since the structures with steel braces have the same period as the corresponding structures with superelastic SMA braces, a good comparison can be made on the effectiveness of using the proposed innovative bracing system in place of a traditional one.

### 8.1. A case study: ground motion LA6

We now present some response results relative to the three-storey frame undergoing ground motion LA6 scaled to a value of PGA of 0.67 *g*. The record in question is the 1979 Imperial Valley earthquake and its original acceleration time-history can be seen in Fig. 6. Also, as Figs. 9 and 10 indicate, it provides the strongest effects

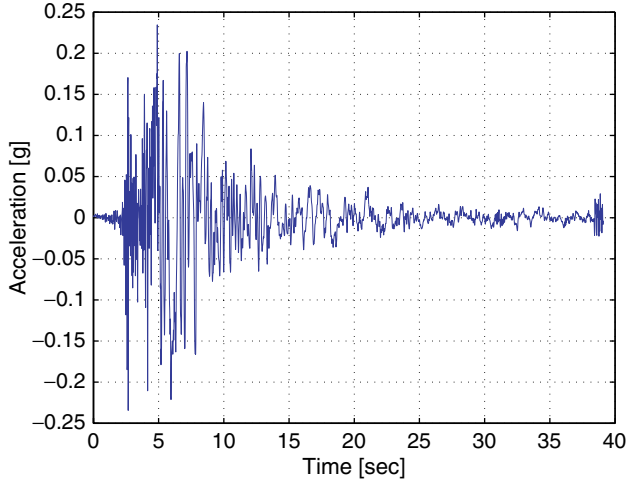


Fig. 6. Ground motion LA6.

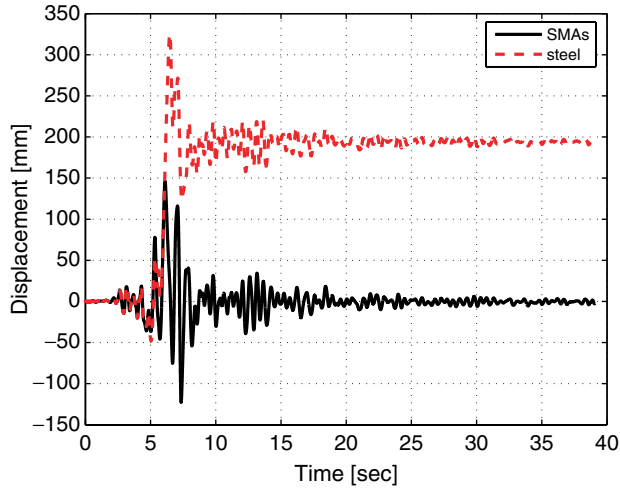


Fig. 7. Displacement time-history exhibited by the top floor of the three-storey frame equipped with either buckling-restrained steel braces or superelastic SMA braces undergoing ground motion LA6 scaled to a value of PGA of  $0.67g$ .

(i.e. maximum interstorey drift and residual drift of approximately 4% and 1.6% respectively) on the considered structure when it is equipped with a traditional bracing system consisting of buckling-restrained steel braces. For brevity, we only consider the three-storey frame since for the six-storey frame similar considerations apply. Attention is focused on both the displacement time-history (Fig. 7) of the top floor and the force-displacement relationship (Fig. 8) exhibited by the lower left brace.

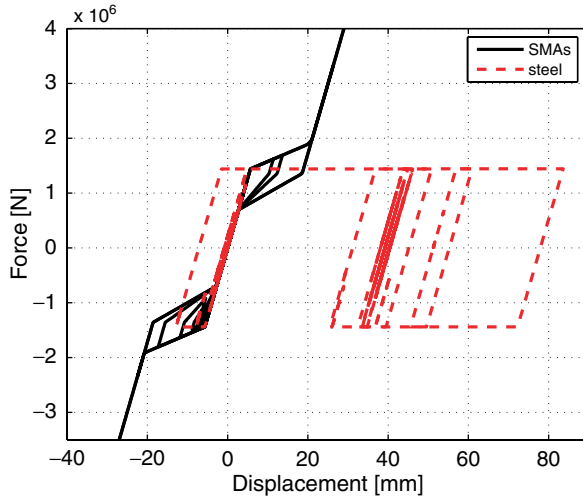


Fig. 8. Force-displacement relationship exhibited by the lower left brace installed in the three-storey frame undergoing ground motion LA6 scaled to a value of PGA of 0.67  $g$ . Note the different hysteresis loops between structural steel and superelastic SMAs.

- Under this record, and considering the two analysed bracing configurations, we observe large differences in terms of maximum displacement experienced by the top floor during shaking (Fig. 7). In particular, its value is 325 mm in the case of the frame equipped with traditional steel braces and decreases to 146 mm (approximately 45% reduction) when utilising the proposed bracing system based on SMAs. Despite the fact that severe inelastic actions occur during the considered seismic event, the superelasticity exhibited by SMAs makes these materials very effective in reducing earthquake-induced vibrations. However, it should be noted that the resulting deformations in the SMAs were in the range of approximately 8% strain which would typically exceed the range for the completion of the A-S transformation. This would result in the commencement of the yielding of the martensite and larger displacements.
- The superelastic SMA braces provide excellent performance in reducing the residual displacement of the top floor, with a computed final value of only 2.5 mm. From Fig. 7, we can also note the significant value of residual displacement (approximately 192 mm) occurred when using traditional steel braces.
- As highlighted in Fig. 8, typical structural steel and superelastic SMAs display completely different hysteresis mechanisms. Steel braces allow for larger ductility demand with respect to superelastic SMA braces, while dissipating a significant amount of seismic energy due to their wider hysteretic loops. On the other hand, the innovative bracing system shows higher values of axial force due to hardening of the material, which may limit the displacements for unexpected strong earthquakes but, at the same time, may result in large shear forces transmitted to beams and columns.

### 8.2. Steel braces versus superelastic SMA braces

Outcomes from the overall study lead to the following main conclusions:

- By observing Fig. 9, which is related to the three-storey frame, we notice that superelastic SMA braces and buckling-restrained steel braces provide similar performance in terms of maximum interstorey drift. In particular, its average value is 1.36% if we use superelastic SMA braces and 1.52% in case we use steel braces. Despite the fact that traditional steel braces may account for a much higher energy dissipation capability (i.e. wider hysteresis loops), the recentring property (i.e. ability of the material of returning back to its initial configuration after the external load is removed) of superelastic SMA braces plays a fundamental role in reducing the structural oscillations. Once again, it should be noted that the strain levels in a few of the cases exceeded the strain limit for the A-S transformation, which would result in the yielding of the martensite. However, in general, most of the cases had strain levels that were less than this value.
- In the six-storey frame (Fig. 11), the innovative bracing system shows better behaviour and a more uniform distribution of the maximum interstorey drift for all the considered seismic inputs. More precisely, its average value decreases of approximately 20% (from 1.35% when using steel braces to 1.08% when using superelastic SMA braces) with respect to the case in which the frame is endowed with a traditional bracing system.
- As far as the residual drift of the top floor is concerned (Figs. 10 and 12), results highlight that in most of the cases superelastic SMA braces have a much better performance than buckling-restrained steel braces. The property

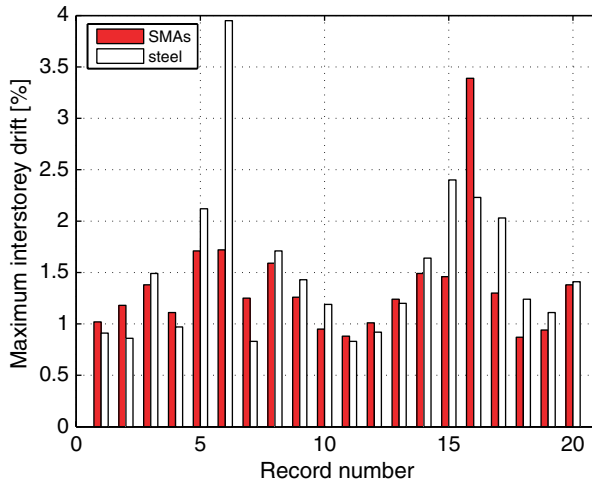


Fig. 9. Maximum interstorey drift exhibited by the three-storey frame equipped with either buckling-restrained steel braces or superelastic SMA braces.

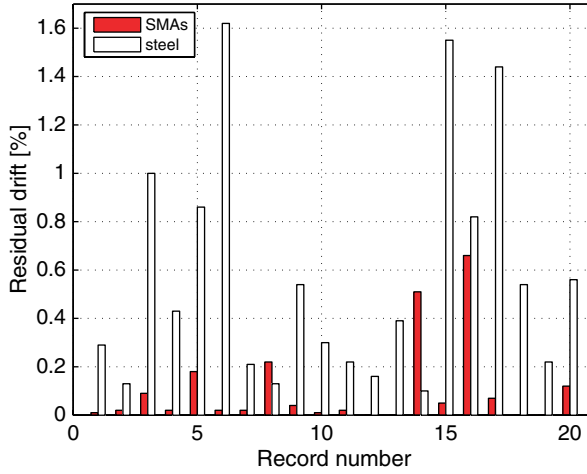


Fig. 10. Residual drift of the top floor exhibited by the three-storey frame equipped with either buckling-restrained steel braces or superelastic SMA braces.

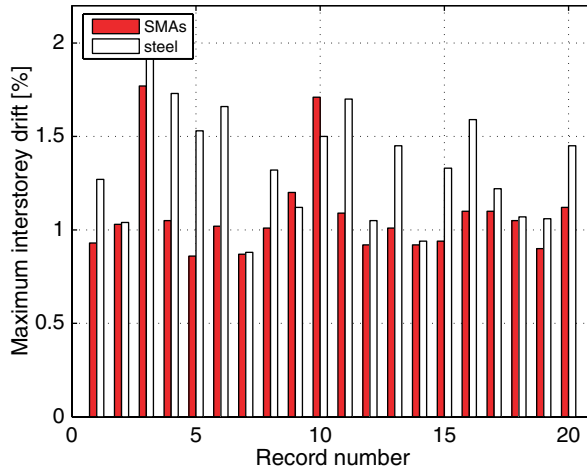


Fig. 11. Maximum interstorey drift exhibited by the six-storey frame equipped with either buckling-restrained steel braces or superelastic SMA braces.

of superelasticity guarantees structural recentering and the superelastic bars are able to bring the structure back to its undeformed shape after the ground motion is over. As a consequence, the permanent deformation in other steel members is strongly reduced even in the case where yielding occurs in the columns.

- Numerical tests related to the three-storey frame undergoing record LA14 and to the six-storey frame undergoing records LA3 and LA10, show that the damage level occurred at the top floor of both structures (Figs. 10 and

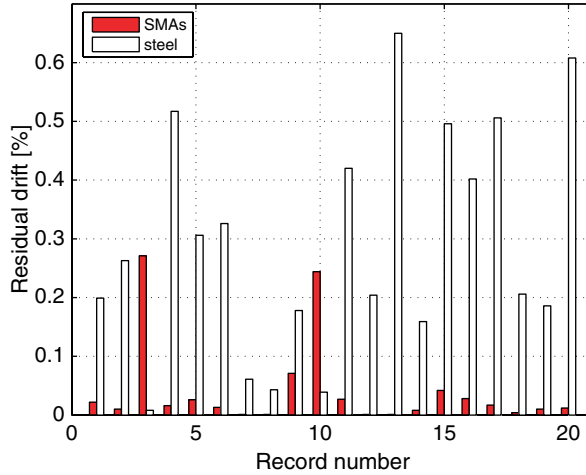


Fig. 12. Residual drift of the top floor exhibited by the six-storey frame equipped with either buckling-restrained steel braces or superelastic SMA braces.

12) is higher if we adopt the new bracing system in place of the traditional one. This is probably due to the post-inelastic behaviour (i.e. branch observed at the end of the upper plateau) of the Nitinol braces, which in their fully martensitic phase transmit high values of forces to columns and/or beams with consequent structural problems caused by yielding. This is, in fact, a limitation of the model since the true behaviour of a SMA material would show a third softening branch after yielding of the martensite.

## 9. Conclusions

This paper focuses on the possibility of using large diameter superelastic Nitinol bars as an innovative bracing system for steel structures. A uniaxial constitutive model for superelastic SMAs is implemented into the finite element software OpenSees and a number of numerical analyses are performed considering one three- and one six-storey steel frame. The dynamic performance of different bracing systems, buckling-restrained steel braces versus superelastic SMA braces, is then evaluated.

The results obtained show that superelastic SMA elements can be successfully used as an innovative bracing system in steel buildings because of their ability to reduce the interstorey drift. Moreover, the property of superelasticity guarantees structural recentering by strongly reducing the residual drift as well as by providing some damping to earthquake-induced vibrations. However, the present numerical study also highlight some limitations in using such innovative technology. In particular, the assumption of a rigid link between the structure and the SMA members is a critical issue because it controls the overall stiffness. Also, the high force levels

transmitted by the superelastic braces in fully martensitic phase may cause yielding problems to beams, columns and connections. As a consequence, a careful design of the connecting elements should be done to ensure adequate performance of the system.

Further research needs to be conducted in order to simulate the actual rate-dependent behaviour of SMA elements. However, this is not expected to change the overall trends or conclusions of the presented study.

### Acknowledgements

The authors would like to thank the financial support of the Italian National Civil Protection Department which, through its Servizio Sismico Nazionale section, provided a scholarship to the second author of this paper. Also, the financial support of the Ministero dell'Istruzione, dell'Università e della Ricerca (MIUR) through the research programs "Shape-memory alloys: constitutive modelling, structural analysis and design of innovative biomedical applications" and "Shape-memory alloys: constitutive modeling, structural behaviour, experimental validation and applicability to innovative biomedical applications" is kindly acknowledged. Additional funding was provided by PECASE Program of the National Science Foundation under grant 0093868.

### References

- Adachi, Y. and Unjoh, S. [1999] "Development of shape memory alloy damper for intelligent bridge systems," *Proceedings of SPIE*, Newport Beach, California, USA **3671**, 31–42.
- Andrawes, B., McCormick, J. and DesRoches, R. [2004] "Effect of cycling modeling parameters on the behavior of shape memory alloys for seismic applications," *Proceedings of SPIE*, San Diego, California, USA.
- Auricchio, F. and Sacco, E. [1997] "A one-dimensional model for superelastic shape-memory alloys with different elastic properties between austenite and martensite," *International Journal of Non-Linear Mechanics* **32**, 1101–1114.
- Baratta, A. and Corbi, O. [2002] "On the dynamic behaviour of elastic-plastic structures equipped with pseudoelastic SMA reinforcements," *Computational Materials Science* **25**, 1–13.
- Bernardini, D. and Brancaloni, F. [1999] "Shape memory alloys modelling for seismic applications," *Proceedings of the Final Workshop of MANSIDE Project — Memory Alloys for New Seismic Isolation and Energy Dissipation Devices*, Roma, Italy, pp. 73–84.
- Bruno, S. and Valente, C. [2002] "Comparative response analysis of conventional and innovative seismic protection strategies," *Earthquake Engineering and Structural Dynamics* **31**, 1067–1092.
- Castellano, M. G. [2000] "Shaking table tests of masonry façade walls with and without SMADs," *Proceedings of the Final Workshop of ISTECH Project — Shape Memory Alloy Devices for Seismic Protection of Cultural Heritage Structures*, Ispra, Italy, pp. 99–109.

- Clark, P. W., Aiken, I. D., Kelly, J. M., Higashino, M. and Krumme R. C. [1995] "Experimental and analytical studies of shape memory alloy dampers for structural control," *Proceedings of SPIE*, San Diego, California, USA **2445**, 241–251.
- Corbi, O. [2003] "Shape memory alloys and their application in structural oscillations attenuation," *Simulation Modelling Practice and Theory* **11**, 387–402.
- Croci, G., Bonci, A. and Viskovic, A. [2000] "Use of shape memory alloy devices in the Basilica of St. Francis of Assisi," *Proceedings of the Final Workshop of ISTECH Project — Shape Memory Alloy Devices for Seismic Protection of Cultural Heritage Structures*, Ispra, Italy, pp. 110–133.
- DesRoches, R. and Delemont, M. [2002] "Seismic retrofit of simply supported bridges using shape memory alloys," *Engineering Structures* **24**, 325–332.
- DesRoches, R., McCormick, J. and Delemont, M. [2004] "Cyclic properties of superelastic shape memory alloy wires and bars," *Journal of Structural Engineering* **130**, 38–46.
- DesRoches, R. and Smith, B. [2004] "Shape memory alloys in seismic resistant design and retrofit: a critical review of their potential and limitations," *Journal of Earthquake Engineering* **8**, 415–429.
- Dolce, M. and Cardone, D. [2001] "Mechanical behaviour of shape memory alloys for seismic applications 2. Austenite NiTi wires subjected to tension," *International Journal of Mechanical Sciences* **43**, 2657–2677.
- Dolce, M., Cardone, D. and Marnetto, R. [2000] "Implementation and testing of passive control devices based on shape memory alloys," *Earthquake Engineering and Structural Dynamics* **29**, 945–968.
- Dolce, M., Cardone, D., Ponzio, F. C. and Valente, C. [2005] "Shaking table tests on reinforced concrete frames without and with passive control systems," *Earthquake Engineering and Structural Dynamics* (in press).
- Duerig, T., Melton, K., Stokel, D. and Wayman, C. [1990] *Engineering Aspects of Shape Memory Alloys* (Butterworth-Heinemann, London).
- Fugazza, D. [2003] *Shape-memory Alloy Devices in Earthquake Engineering: Mechanical Properties, Constitutive Modelling and Numerical Simulations*, Master's thesis, European School for Advanced Studies in Reduction of Seismic Risk (ROSE School), Pavia, Italy.
- Fugazza, D. [2005] *Experimental Investigation on the Cyclic Properties of Superelastic NiTi Shape-memory Alloy Wires and Bars*, Individual study, European School for Advanced Studies in Reduction of Seismic Risk (ROSE School), Pavia, Italy.
- Han, Y.-L., Li, Q. S., Li, A.-Q., Leung, A. Y. T. and Lin, P.-H. [2003] "Structural vibration control by shape memory alloy damper," *Earthquake Engineering and Structural Dynamics* **32**, 483–494.
- Indirli, M. [2000] "The demo-intervention of the ISTECH Project: the Bell Tower of S. Giorgio in Trignano (Italy)," *Proceedings of the Final Workshop of ISTECH Project — Shape Memory Alloy Devices for Seismic Protection of Cultural Heritage Structures*, Ispra, Italy, pp. 134–146.
- Indirli, M., Carpani, B., Martelli, A., Castellano, M. G., Infanti, S., Croci, G., Biritognolo, M., Bonci, A., Viskovic, A. and Viani, S. [2000] "Experimental tests on masonry structures provided with shape memory alloy antiseismic devices," *12th World Conference in Earthquake Engineering*, Auckland, New Zealand, pp. 1–8.
- Krumme, R., Hayes, J. and Sweeney, S. [1995] "Structural damping with shape-memory alloys: one class of devices," *Proceedings of SPIE*, San Diego, California, USA **2445**, 225–240.
- Mazzolani, F. M. and Mandara, A. [2002] "Modern trends in the use of special metals for the improvement of historical and monumental structures," *Engineering Structures* **24**, 843–856.

- Mazzoni, S., McKenna, F., Scott, M. H., Fenves, G. L. and Jeremic, B. [2003] *Open System for Earthquake Engineering Simulation (OpenSees) — Command Language Manual*.
- Ocel, J., DesRoches, R., Leon, R. T., Hess, W. G., Krumme, R., Hayes, J. R. and Sweeney, S. [2004] “Steel beam-column connections using shape memory alloys,” *Journal of Structural Engineering* **130**, 732–740.
- Sabelli, R. [2001] “Research on improving the design and analysis of earthquake-resistant steel-braced frames,” *The 2000 NEHRP Professional Fellowship Report*.
- Sabelli, R., Mahin, S. and Chang, C. [2003] “Seismic demands on steel braced frame buildings with buckling-restrained braces,” *Engineering Structures* **25**, 655–666.
- Valente, C., Cardone, D., Lamonaca, B. G. and Ponzo, F. M. [1999] “Shaking table tests of structures with conventional and SMA based protection devices,” *Proceedings of the Final Workshop of MANSIDE Project — Memory Alloys for New Seismic Isolation and Energy Dissipation Devices*, Roma, Italy, pp. 177–194.
- Wilde, K., Gardoni, P. and Fujino, Y. [2000] “Base isolation system with shape memory alloy device for elevated highway bridges,” *Engineering Structures* **22**, 222–229.
- Wilson, J. and Wesolowsky, M. [2005] “Shape memory alloys for seismic response modification: a state-of-the-art review,” *Earthquake Spectra* **21**, 569–601.